Hindawi Publishing Corporation
Journal of Nanomaterials
Volume 2008, Article ID 659397, 10 pages
doi:10.1155/2008/659397

Research Article

Improving the Performance of Lithium-Ion Batteries by Using Spinel Nanoparticles

J. C. Arrebola, A. Caballero, L. Hernán, and J. Morales

Departamento de Química Inorgánica e Ingeniería Química, Universidad de Córdoba, Campus de Rabanales, Edificio Marie Curie, 14071 Córdoba, Spain

Correspondence should be addressed to L. Hernán, iq1hepal@uco.es

Received 31 July 2007; Revised 21 January 2008; Accepted 10 March 2008

Recommended by Jun Lou

In this work, we examined the use of nanospinels to construct batttery electrodes. We chose two spinels suitable as cathode materials ($LiMn_2O_4$ and $LiNi_{0.5}Mn_{1.5}O_4$, which are representative of 4 and 5 V versus Li metal, resp.) and one providing good results as anode ($Li_4Ti_5O_{12}$). In order to ensure good cell performance, nanometric particles must meet another requirement; thus they should contain few surface or bulk defects (i.e., they should be highly crystalline). Because the synthesis of such spinels usually requires a thermal treatment, ensuring that they will meet both requirements entails accuratly controlling in the synthesis conditions. Thermal decomposition of nanooxalate in the spinel-conaining elements obtained by mechanochenical activation in the presence of polymers provides a simple, effective route for this purpose. We prepared two types of hybrid lithium-ion batteries using $LiMn_2O_4$ and $LiNi_{0.5}Mn_{1.5}O_4$ as cathode materials, and $Li_4Ti_5O_{12}$ as anode material. The electrochemical properties of these cells were compared with those of a similar configuration made from micrometric particles. The nano-nano configuration exhibited higher reversibility and better performance than the micro-micro configuartion in both types of cells, possibly as a result of lithium ions in the former being able to migrate more easily into the electrode material.

1. INTRODUCTION

Some properties of nanometric materials differ markedly from those of micrometric materials of identical composition by effect of mere simple size effects or differences in electronic structure. This has aroused great expectations in many fields including the production of electrochemical energy storage systems. Thus, the use of nanometric materials to prepare electrodes for lithium-ions batteries has gained substantial interest in the last few years [1–6]. Trivial size effects (e.g., an increased surface-to-volume ratio and shorter length displacements for lithium ions) can lead to an improved rate capability and cycle life of cells.

On the other hand, the increased surface area of the electrode and also the increased area of the electrode/electrolyte interface provide additional advantages for nanometric particles over the bulk material [7] such as (i) an improved reaction kinetics that increases the extent of development and reversibility of the lithium insertion/extraction process and results in increased cell capacity and better capacity retention, and (ii) the ability to use high charge/discharge rates. However, the increased reactivity of nanometric materials can raise some problems derived from a greater vulnerability to attack by the electrolyte (particularly at low charge/discharge rates). Under these conditions, the lithium insertion/extraction process takes a long time and contact between the active material and electrolyte prolonged. This situation can be detrimental when the electrolyte is capable of decomposing the electrode. Such is the case with the release of HF from $LiPF_6$ promoted by the presence of water traces. Coating particle surfaces with a protective agent can help overcome this drawback [8]. However, the main disadvantage of nanometric materials is probably the typical labour intensity and high cost of their synthetic procedures. Developing simple affordable synthetic methods will be one of the keys for nanometric materials to prevail in the design of electrochemical devices for energy storage and conversion.

Another valuable property of lithium-ion batteries is their ability to operate at the highest availablevoltages. Provided cells retain their capacity, this can be used to increase their specific energy. Cell voltage is determined by the difference in Li chemical potential between the two

insertion electrodes. The greater the difference is, the higher will be the cell voltage. This can be accomplished by using anodic and cathodic materials with the lowest and highest potentials versus the lithium reference electrode, respectively. The presence of Li ions that can be extracted during charging and inserted on discharging the cell is an indispensable condition for cathodic materials to be active in this respect. The most attractive and widely studied compounds in this context are the layered oxide $LiCoO_2$ [9] (commercial lithium-ion batteries are based on it, but its high cost and toxicity can compromise its leading position), and the spinel $LiMn_2O_4$, which is more inexpensive and environmentally benign than $LiCoO_2$ but has poorer cycling properties [10]. The spinel gains stability when Mn is partly replaced with other elements such as V [11], Cr [12], Fe [13], Co [14], Cu [15], or Ni [16]. A spinel of composition $LiNi_{0.5}Mn_{1.5}O_4$ has been prepared which affords complete reversible extraction of Li^+ at ca. 4.7 V (i.e., more than 0.5 V above the potential for the unsubsituted spinel). This compound has started a new generation of lithium-ion batteries capable of operating at higher voltages.

All these compounds share a common feature: introducting Li^+ in their structures usually requires a thermal treatment. Hence, the most common procedure used for their synthesis in nanometric size is based on combustion [17]. There is, however, an alternative procedure alike to a ceramic method which starts from nanometric precursors and involves a rapid heating. The preparation of nanometric precursors, which can be obtained by mechanochemical activation at room temperature [18], is a key factor. Activation in the presence of a polymer provides highly crystalline nanoparticles [19], otherwise it is difficult to obtain with other methods that require prolonged heating and/or higher heating temperatures.

Polymer-assisted nanoparticles possess significant advantages, namely, (i) they are more resistant to electrolyte attack than are those obtained in the absence of polymer, probably because of lower crystallinity, and (ii) they exhibit a better electrochemical response when operated in the voltage window close to 5 V. All these factors combine to give nanocompounds which can be cycled at high currents [20]. This was comfirmed here by highly crystalline Li-containing nanospinels (viz. $LiMn_2O_4$ and $LiNi_{0.5}Mn_{1.5}O_4$, which were used as cathode materials and $Li_4Ti_5O_{12}$ as anode material). The hybrid lithium batteries made from these compounds were found to exhibit good performance under a wide range of charge/discharge rates.

2. EXPERIMENTAL

The above-describe synthetic method is effective for any Li-containing oxide. We prepared the following spinels in this work: $LiMn_2O_4$ (LMO), $Li_4Ti_5O_{12}$ (LTO), and $LiNi_{0.5}Mn_{1.5}O_4$ (LNMO). In previous work [21], the method was used to prepare of $LiCoO_2$ and $LiNi_{0.5}Mn_{0.5}O_2$ layered oxides. The method is based on the synthesis of nanometric oxalates followed by rapid calcination up to 800°C at a high heating rate (ca. 20°C/min). Then, the furnace is shutoff, and the material is allowed to cool to room temperature inside. The formation of nanometric oxalate is boosted by the presence of highly hydrated precursors in excess oxalic acid dihydrate. Mechanical activation was done in a planetary high-energy ball mill in the air at room temperature in two steps, first under dryness for 15 minutes and then in ethanol for another 15 minutes. This sufficed to obtain oxalate particles less than 10 nm in size.

Mechanical activation can be done in the presence of a polymer in order to tailor particle size and shape. Two polymers were tested: polyethyleneglycol (PEG) in molecular weight 400 and polymethylmethacrylate (PMMA). Mechanical activation for 1 hour sufficed to obtain a homogeneous mixture of polymer and precursors. Further heating at 800°C yielded highly crystalline nanoparticles.

X-ray diffraction (XRD) patterns were recorded on a Siemens D5000 X-ray diffractometer using nonmonochromated Cu Kα radiation and a graphite monochromator for the diffracted beam. Thermogravimetric measurements were made under ambient conditions, using a Cahn 2000 thermobalance at a heating rate of 10°C/min. Transmission electron microscopy (TEM) images were obtained with a Phillips TEM operating at 100 keV and SEM images with a Jeol 6400 scanning electron microscope.

Electrochemical measurements were carried out with CR2032 two-electrodecoin cells supplied by Hohsen Corporation. Powdered pellets 13 mm in diameter were prepared by pressing, in a stainless steel grid, ca. 10 mg of active material with acetylene black (15 wt%). The electrolyte, supplied by Merck, was 1 M anhydrous $LiPF_6$ in a 1 : 1 mixture of ethylene carbonate and dimethyl carbonate. Cells were assembled in an M-Braun glovebox. Cycling tests were performed on a McPile II (biologic) potentiostat-galvanostat system under a galvanostatic regime. The Li-ion batteries were anode limited [22], and the specific capacity and rate of the batteries referred to the mass of the negative electrode.

3. RESULTS AND DISCUSSION

3.1. Morphological properties

As stated above, thermal treatment of an appropriate precursor for a short time provides a simple route for obtaining an Li-containing oxide of nanometric size. The suitability of the precursor is a key factor here. We started from hydrated acetates (except for the synthesis of $Li_4Ti_5O_{12}$, where the Ti source was acetylacetonate). On contact with oxalic acid dihydrate and mechanochemical activation, the acetates become nanometric oxalates (see Figure 1). The increased reactivity of these oxalates compared with micrometric particles affords the use of milder thermal conditions to obtain the spinel framework. The combination of TG curves and XRD patterns revealed that the spinel is formed at 400°C, albeit with low crystallinity. Heating at 800°C for a short time results in improved particle crystallinity as revealed the reduction in the broadening of the X-ray diffraction lines. Figure 2 shows some XRD patterns representative of the different conditions used in the spinel synthesis. At this temperature, the spinel peaks are quite well resolved, and peaks assigned to transition metal oxide-based impurities are

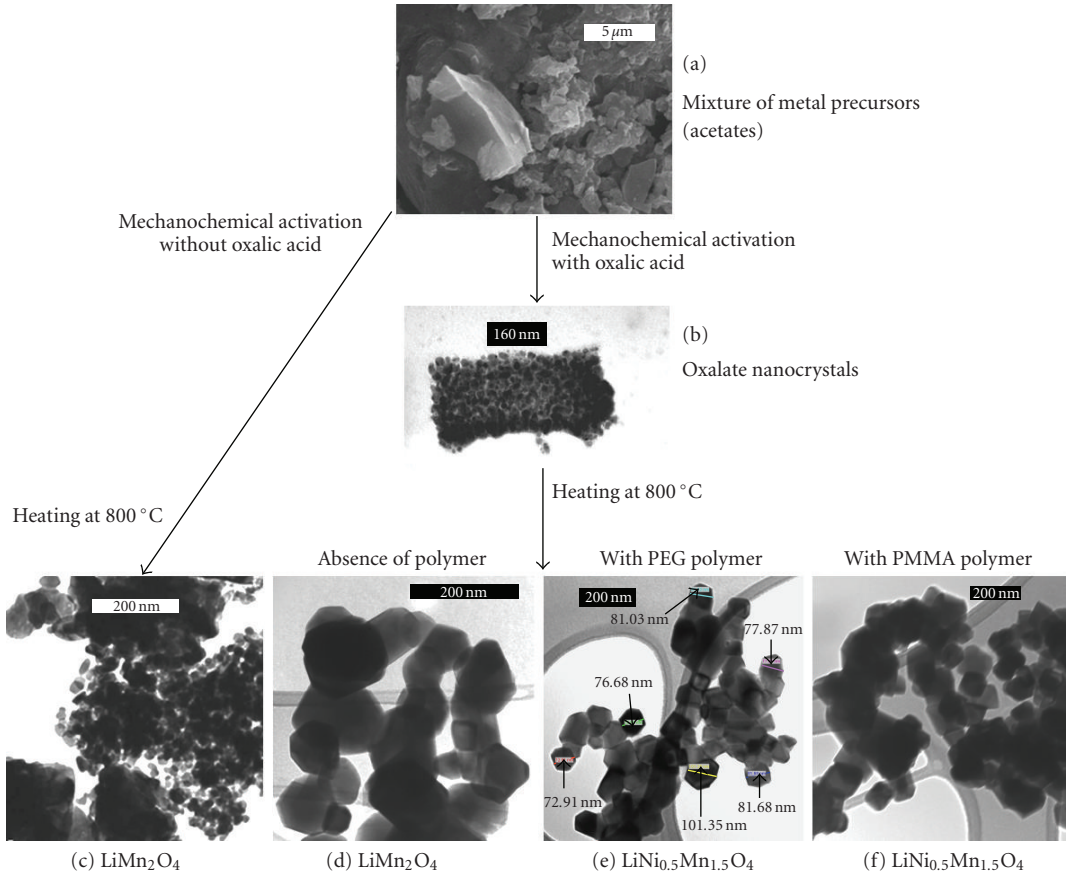

Figure 1: Steps of the method used to synthesize the nanospinels.

hardly perceptible. The role played by oxalic acid is shown in Figures 1(c) and 1(d). The presence of oxalic acid dihydrate in the medium plays a key role in the final particle size of the mixed oxide by means of the formation of oxalate nanocrystals on grinding (see Figure 1(b)). Nucleation and growth of these reaction products are facilitated by the presence of hydration water. Thus, this precursor-like route enhances the uniform distribution of the elements resulting in a well-defined morphology and quite homogeneous particle size. By contrast, direct synthesis from the acetates in the absence of oxalic acid resulted in wider particle size distribution and nanoparticles coexisted with microparticles (see Figure 1(c)).

The use of polymers in the synthetic procedure has two main effects, namely, (i) particle size is reduced (compare Figures 1(d), 1(e), and 1(f)) and (ii) an improvement in spinel crystallinity, as shown below. The polymer helps to adopt a more homogeneous distribution of metal ions on an atomic scale as a result of its ability to coordinate to the metal ions forming the spinel. The functional groups of the polymer capable of acting as Lewis basic sites—atoms with nonbonding electron pairs—may bind to the ions, thereby bringing them closer and shortening diffusion paths to adopt the spinel framework. This model is consistent with the results obtained by using a polymer such as poly(divydilene fluoride) (PVDF), where no functional oxygen atoms are present, with which the spinel synthesis failed. Thus, the functional groups of the polymer are key factors for the spinel synthesis and should be able to approach and stabilize the metal ions via their chelating properties. Thus, the presence of the polymer, in addition to tailoring the particle shape, helps maintain connectivity between nanocrystals, thereby facilitating the release of strains as the temperature is raised. Nanoparticles adopt a well-defined octahedral morphology typical of the spinel structure (see Figure 3(a)). Also, lattice defects are insignificant as revealed by HREM images (see Figure 3(b)). The interplanar spacing was calculated to be ca. 0.46, which corresponds to the orientation of (111) atomic planes. The high crystallinity observed by TEM, a highly localized technique, was confirmed from X-ray broadening analysis, more suitable to examine bulk properties of a material. The lattice distortion was estimated from the full width at half maximum (FWHM), using the Williamson and Hall equation [23]:

$$\beta \cos\theta = \frac{2\langle e\rangle \operatorname{sen}\theta + 0.9\lambda}{D}, \tag{1}$$

where β is the integral breadth after correction for instrumental broadening from highly crystalline quartz and kα_2 elimination using the Rachinger method [24], $\langle e\rangle$ denotes

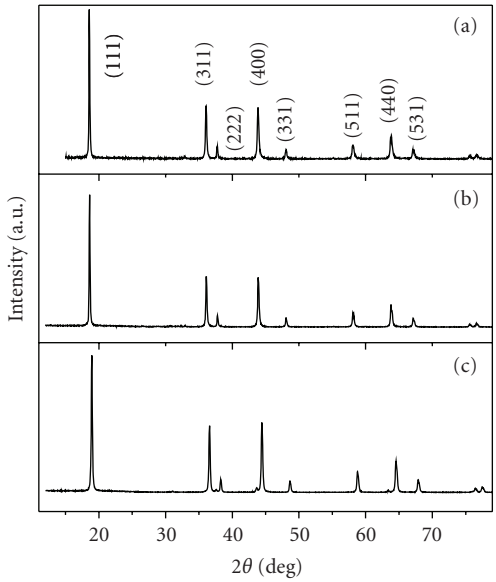

Figure 2: XRD patterns for the spinels. Samples: (a) and (b) $LiMn_2O_4$ in the absence and presence of oxalic acid, (c) $LiNi_{0.5}Mn_{1.5}O_4$ in the presence of oxalic acid and PEG400.

local strains (defined as $\Delta d/d$, where d is the interplanar space), and D is crystallite size. Equation (1) was applied to the strongest reflections that do not overlap with other reflections. Figure 4 shows the plots of the above equation for different spinels, and Table 1 lists the crystallite sizes and strains calculated from the intercepts and slopes, respectively. Both the presence of oxalic acid and especially polymer in the synthesis improved particle crystallinity as microstrain content decreased under these conditions. The lower crystallite size for the $LiMn_2O_4$ spinel prepared in the absence of oxalic acid compared with that of the same spinel obtained in the presence of oxalic acid could be due to the wider particle size distribution of the former sample. Figure 1(c) shows the presence of ill-defined particles of few tens nanometer with others exceeding 200 nm. In any case, highly crystalline particles of small size are quite appropriate to cycle at high charge/discharge rates as Li-ion displacement is enhanced by effect of the reduced probability to find defects potentially truncating their movement.

3.2. Electrochemical properties

3.2.1. Nanometric $LiMn_2O_4$ versus Li

The essential condition for a material to be useful in lithium-ion battery cathodes is that it should be able to react in a reversible manner with lithium at high potentials. This requirement is met by the spinel $LiMn_2O_4$, for which a vast amount of literature is available [25]. This spinel can extract and insert lithium above 4 V versus Li. Figure 5 shows the variation of the specific capacity delivered by half-cells made from nanometric particles as a function of the number of cycles. Galvanostatic data were recorded at different charge/discharge rates from C/4 to 4C (C representing 1 Li^+ ion exchanged in 1 hour, equivalent to 148 mA/g). The initial capacities obtained ranged from 108 at C/4 to 100 mAh/g at 4C. The difference in capacity was in fact rather small (8%) in spite of the significant difference in rate (16 times). On further cycling, the half cells exhibited good capacity retention, irrespective of the rate capability used. With the electrode made from micrometric particles, the initial capacity delivered by the half-cell was 107 mAh/g at C/4 and 95 mAh/g at 1C, which is close to the value for the electrode made from nanometric particles. However, capacity fading with cycling was more pronounced than in the half cell made from nanometric particles. The capacity loss was particularly significant at 1C. Under these cycling conditions, the capacity fell from 95 to 40 mAh/g over the first twenty cycles; in the half-cell made from nanometric particles, however, the capacity only decreased from 105 to 100 mAh/g. The origin of this striking behavior may be associated to the way lithium diffusion is affected by particle size. The time τ taken to travel a distance r can be calculated from the equation:

$$\tau = \frac{r^2}{\pi D}, \tag{2}$$

where D is the diffusion coefficient of Li^+. Thus, for nanoscale materials (viz. those having a size of 1−100 nm in at least one direction), Li ions take few minutes to cross nanoparticles (the average value of D for Li^+ is ca. 10^{-4} cm^2/s). Thus, reducing the average diffusion distances delays concentration polarization and allows cells to operate at high currents and hence electrode rate capabilities to be improved [7]. Obviously, reducing the distance for Li^+ ions travel must be also beneficial when the cell anode is made from an insertion electrode, as shown below.

Table 1: Crystallite size and microstrain content of Li-Mn spinels.

Sample	D (nm)	Microstrain ($\times 10^{-4}$)
$LiMn_2O_4$ [(a)]	92	19.3
$LiMn_2O_4$ [(b)]	116	10.7
$LiNi_{0.5}Mn_{1.5}O_4$ [(c)]	79	2.1

Synthesis conditions: [(a)]absence of oxalic acid, [(b,c)]with oxalic acid, [(c)]with PEG400.

3.2.2. Nanometric $LiMn_2O_4$ versus $Li_4Ti_5O_{12}$ (hybrid batteries)

In most commercial batteries the positive and negative electrodes are made from $LiCoO_2$ and graphite, respectively. These components have two major shortcomings. Graphite operates at a very low voltage (ca. 50 mV versus Li). Under these conditions, the electrolyte is thermodynamically unstable and can decompose releasing gases which detract from battery safety. On the other hand, cobalt is a toxic and expensive element. In this context, Li-based spinels provide interesting prospects for circumventing these shortcomings. The spinels $Li_4Ti_5O_{12}$ and $LiMn_2O_4$ are good choices for this purpose as they can act as anode and cathode materials, respectively, for batteries. LTO is one of the few lithium intercalation compounds known that

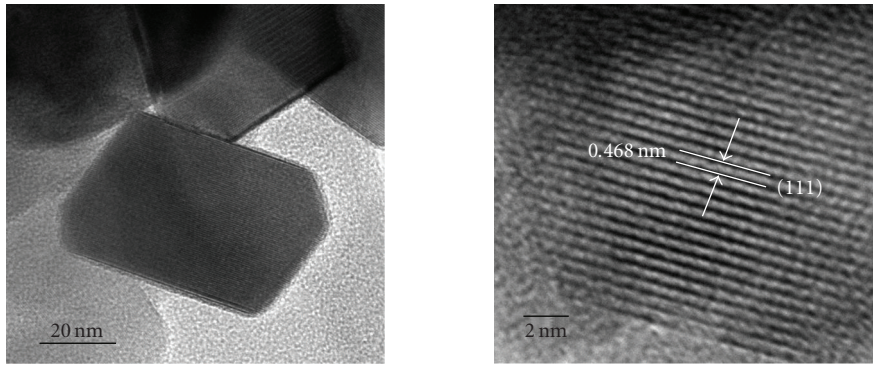

Figure 3: (a) TEM and (b) HREM images of $LiNi_{0.5}Mn_{1.5}O_4$ nanocrystals synthesized in the presence of PEG400.

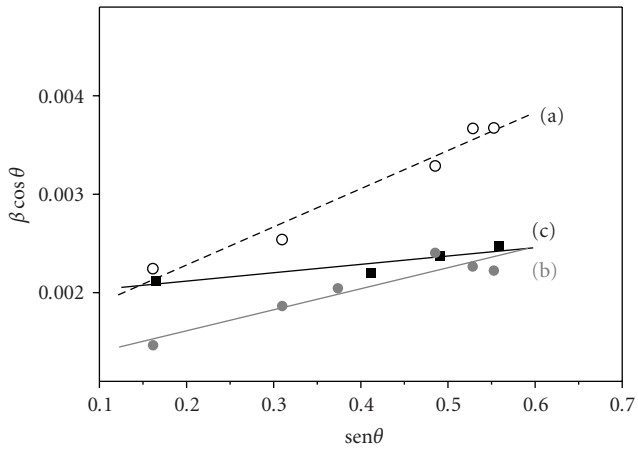

Figure 4: Plots of the Williamson and Hall equation for various (hkl) reflections. Samples calcined at 800°C: $LiMn_2O_4$ in the absence (a,∘) and presence (b,•) of oxalic acid, $LiNi_{0.5}Mn_{1.5}O_4$ in the presence (c, ■) of oxalic acid and PEG400.

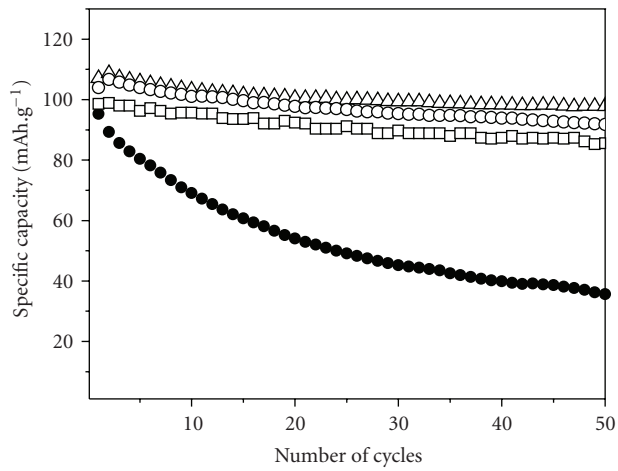

Figure 5: Variation of cell capacity in $LiMn_2O_4$/Li half-cells as a function of the number of cycles. Rate: (Δ) C4, (∘) 1C, (□) 4C, and m-$LiMn_2O_4$/Li half-cell at (•) 1C.

undergoes little expansion or contraction during the lithium insertion/reinsertion process [26]. We have found battery performance to be significantly improved by using both compounds as nanoparticles [27]. Hybrid batteries made from such particles exhibit enhanced rate capabilities and surpass batteries made from larger particles (microparticles) in performance.

Figure 6 shows the charge/discharge curves for two batteries made from the spinels obtained as nano(n)- and micropaticles (m). The curve shapes are typical for $LiMn_2O_4$, with two pseudoplateaux consistent with the two-step mechanism for lithium extraction and insertion [28]. The capacity values delivered by the cells in the 1st and 10th cycle as measured at C/4 and 1C are shown in Table 2.

The initial capacity delivered by the cell was higher when the electrodes were made from nanoparticles, irrespective of the discharge rate used. However, the greater differences were observed at 1C, consistent with the better electrochemical response of nanometric particles cycled at high rates. On cycling at a low rate (C/4), capacity retention of this cell was quite good. By contrast, the capacity of the cell made from microparticles decreased by about a 10%. At higher rates (1C), the capacity of the two batteries faded with cycling, but capacity retention in the battery made from nanoparticles was better (its capacity loss was 10% versus 26%). Clearly, as previously found for the half cell, a nanometric size helps in improving battery performance.

Table 2: Capacity values delivered by the hybrid cells (mAh/g).

Battery	1st discharge		10th discharge	
	C/4	1C	C/4	1C
n-LMO–n-LTO	134	120	133	108
m-LMO–m-LTO	107	76	96	66

3.2.3. *Nanometric $LiNi_{0.5}Mn_{1.5}O_4$ versus Li*

The highest cathode potentials achieved to date are in the region of 5 V versus Li, value which is on the verge of

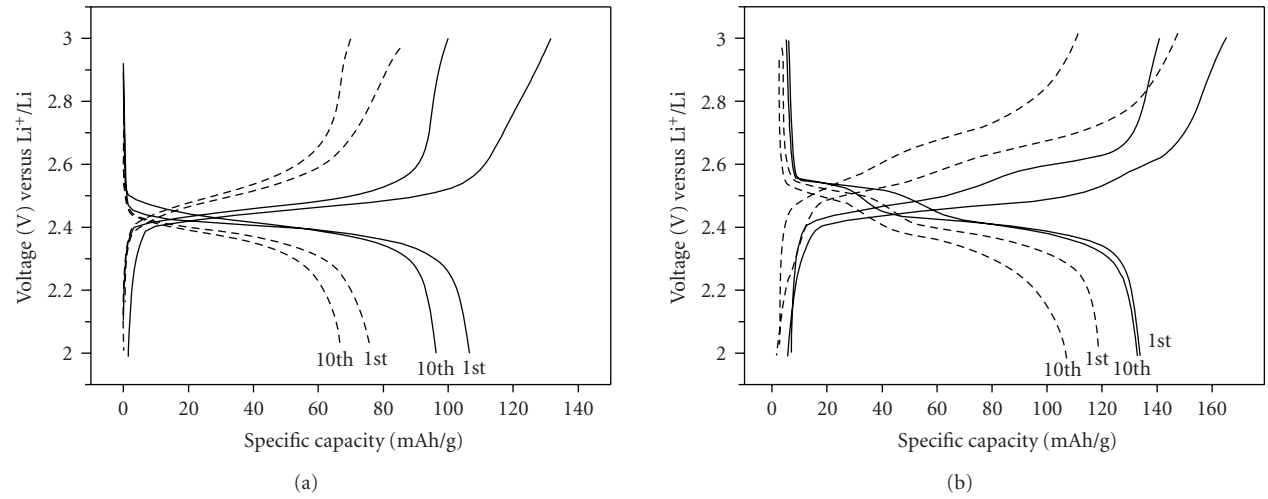

Figure 6: Galvanostatic profiles for the first and tenth charge/discharge of (a) m-$LiMn_2O_4$/m-$Li_4Ti_5O_{12}$ and (b) n-$LiMn_2O_4$/n-$Li_4Ti_5O_{12}$ hybrid batteries. Rates: C4 (solid line) and 1C (dash line).

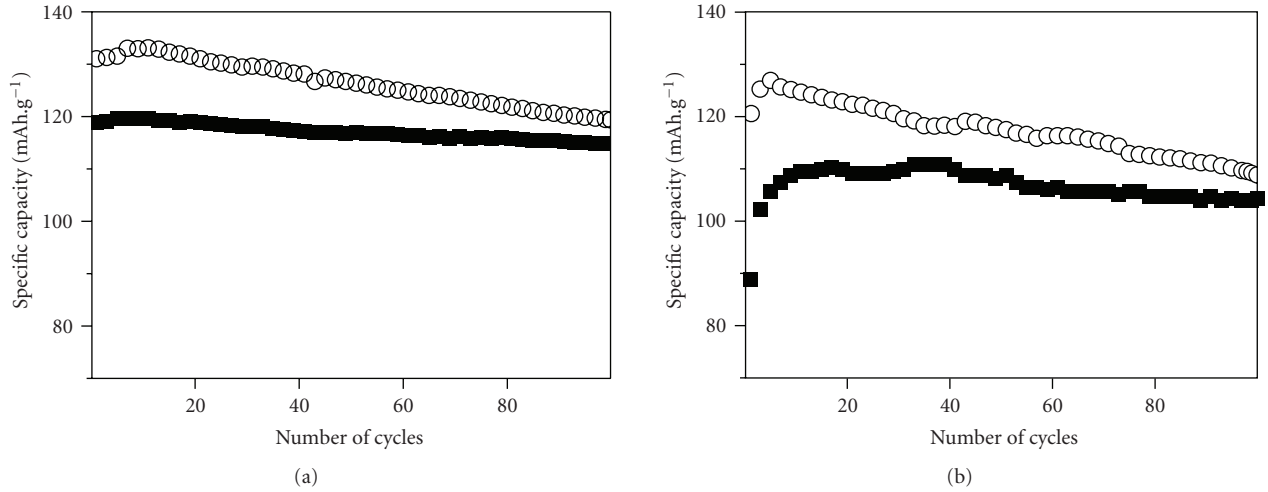

Figure 7: Variation of cell capacity as a function of the number of cycles in half-cells made from m-$LiNi_{0.5}Mn_{1.5}O_4$ spinel (■) and a mixture of 50/50 wt% n-$LiNi_{0.5}Mn_{1.5}O_4$/m-$LiNi_{0.5}Mn_{1.5}O_4$ (○). Charge/discharge rate: (a) C/4, (b) 2C.

the potential window for liquid-based electrolytes. Some Li-based spinels (e.g., $LiNi_{0.5}Mn_{1.5}O_4$) possess this property and are the best candidates for future applications [22]. Li is removed from this compound between 4.5 and 4.8 V, and charge neutrality is maintained by oxidizing Ni^{2+} to Ni^{4+} [29]. In order to ensure good reversibility in the electrochemical reaction at high voltages, the electrode must be made from a highly crystalline spinel. The conditions used to obtain nanometric particles usually provide solids with a high defect content. In other words, particles are poorly crystalline as revealed by X-ray line broadening analysis [19]. This is so because the heating temperature cannot be too high and the heating time should be as short as possible in order to avoid sintering. Spinels prepared as microparticles are not subject to this drawback and possess a high crystallinity. As stated above, however, microparticles exhibit a limited electrochemical response in lithium cells, particularly at high rates. One way of overcoming this restriction is by using composite electrodes made from a mixture of nano- and micrometric particles. In this way, cells can exploit the advantages of nanoparticles (high rate capabilities) and microparticles (good reversibility in the electrochemical reaction).

Figure 7 shows the capacity delivered by various half cells as a function of the number of cycles. Two types of electrodes were studied that were prepared from (i) microparticles and (ii) a 50 : 50 w/w mixture of micro- and nanoparticles (composite electrode) obtained by mechanochemical activation for 15 minutes [30]. Tests were conducted at two different rates (C/4 and 2C). As can be seen, the best performance

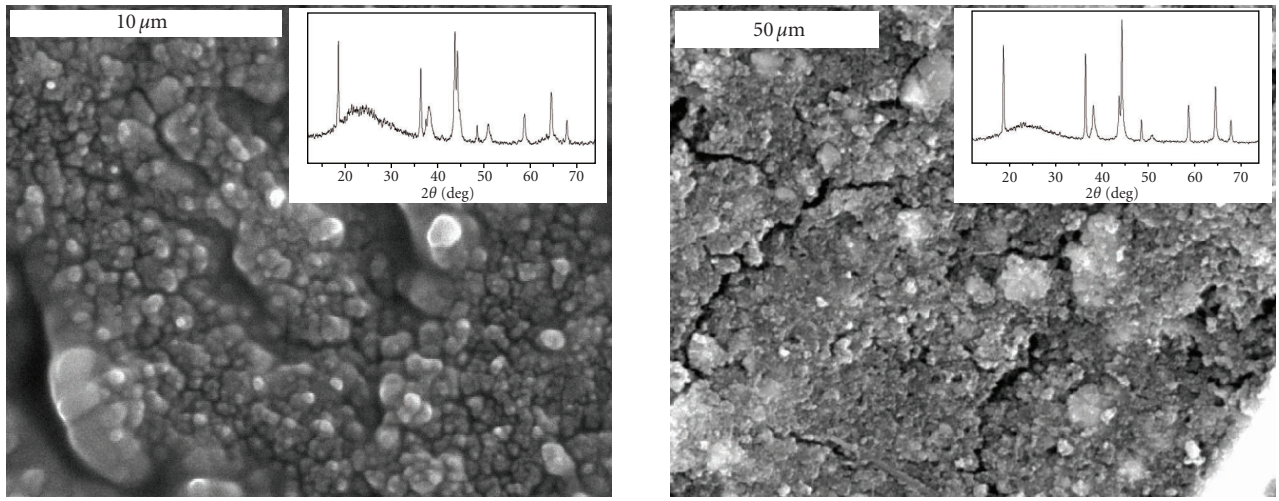

(a) (b)

Figure 8: SEM images of electrodes tested at C/4 after the hundredth discharge. (a) Micrometric spinel and (b) 50/50 composite electrode.

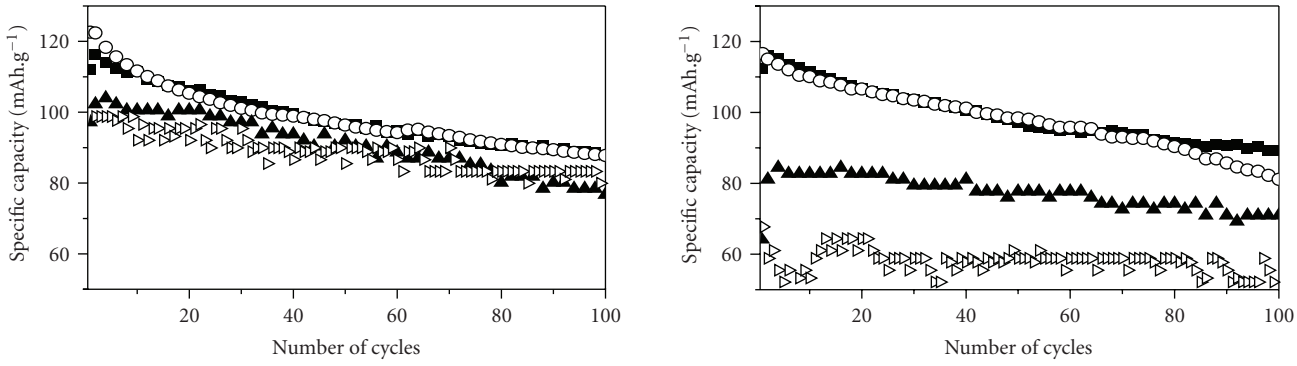

(a) (b)

Figure 9: Variation of cell capacity as a function of the number of cycles at a variable charge/discharge rate. Half-cells made from the n-$LiNi_{0.5}Mn_{1.5}O_4$ spinel prepared in (a) the presence and (b) the absence of PEG-800. Charge/discharge rate: C/4 (■), 2C (∘), 8C (▲), 15C (▷).

was obtained for the composite electrode, irrespective of the charge/discharge rate used. This electrode delivered a higher capacity over the one hundred cycles measured. Differences in textural properties of the electrodes rather than in the structural properties of the spinels seem to be the origin of the enhanced performance of the composite electrode. As can be seen in the insets of Figure 8, the particles maintained the spinel structure with similar unit cell dimensions to those of the pristine compounds on cycling. However, the SEM images (see Figure 8) revealed significant differences between the two electrodes. Thus, the composite electrode was the better at retaining its integrity. Also, it was the electrode exhibiting the best electrochemical performance (see Figure 7(a)). The appearance of the electrode made from the m-spinel (see Figure 7(b)) was quite different. As expected, particles were clearly larger and not so closely bound as in the composite electrode. The nanoparticles probably occupy the cavities formed upon compaction of the microparticles. Therefore, the nanoparticles seem to act as binders between the microparticles, thereby improving connectivity between particles and facilitating transport of charge carriers. This must decrease cell polarization and increase the reversibility of the reaction with lithium, thereby improving cell performance.

As stated above, one alternative route for improving cell performance involves preparing electrodes from highly crystalline nanoparticles. The use of polymers in the synthetic procedure has proved an excellent method for obtaining highly crystalline nanosized spinels. The beneficial effect on their electrochemical properties is apparent from Figures 9(a) and 9(b), which compare the performance of half cells made from nanoparticles of $LiNi_{0.5}Mn_{1.5}O_4$ obtained in the presence and absence of polymer (PEG800). The influence of the charge/discharge rate on the capacity delivered by

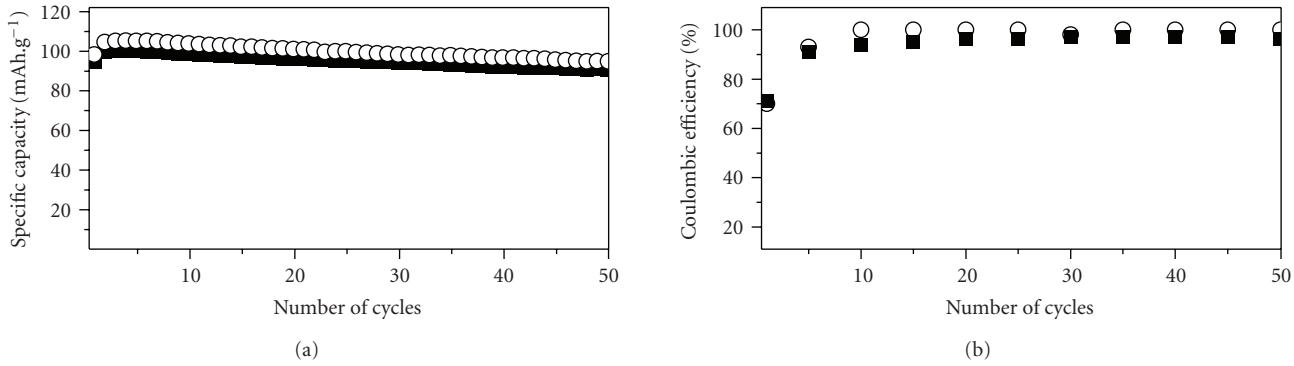

Figure 10: (a) Variation of the specific capacity delivered by the half-cell made from n-$LiNi_{0.5}Mn_{1.5}O_4$ spinel prepared in the presence of PEG-800 under different charge/discharge regimes. (∘) Charge 2C, discharge C/4; (■) charge 4C, discharge C/4. (b) Coulombic efficiency.

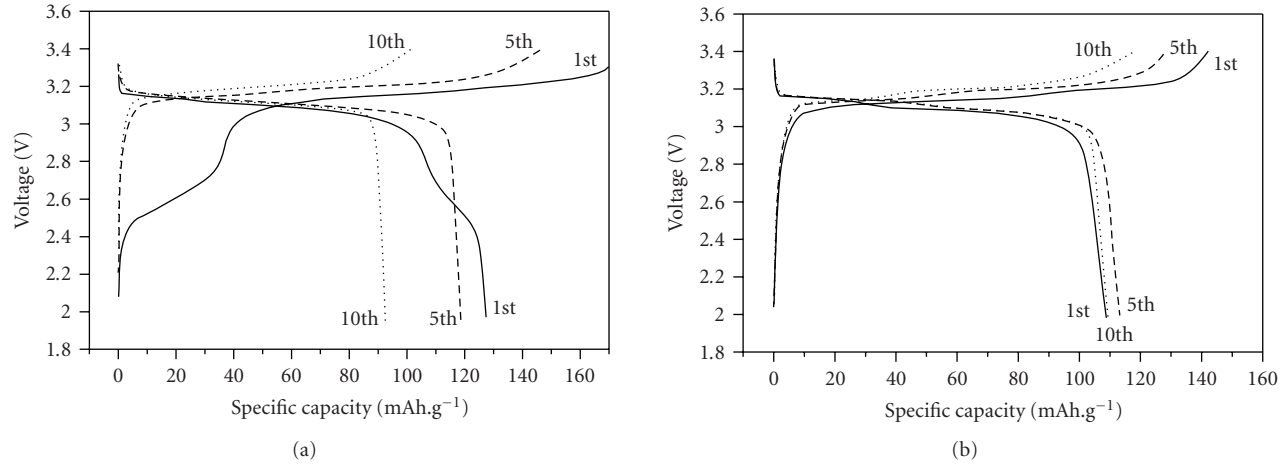

Figure 11: Galvanostatic profiles for the first (solid line), fifth (dash line), and tenth (dot line) charge/discharge of (a) m-$LiNi_{0.5}Mn_{1.5}O_4$/m-$Li_4Ti_5O_{12}$ and (b) n-$LiNi_{0.5}Mn_{1.5}O_4$/n-$Li_4Ti_5O_{12}$ hybrid batteries.

the half-cells is weaker when the electrode is prepared from nanoparticles obtained in the presence of polymer. The initial capacity values range from 120 at C/4 to 100 mAh/g at 15C. In the electrode made from the nanospinel obtained in the absence of polymer, the delivered capacity shifts from 120 to 60 mAh/g. Although particle size was similar for the two spinels, the use of a polymer facilitated the release of defects and internal strains, thereby incrasing the crystallinity of the nanoparticles [31].

Another interesting property of the cells made from nanometric $LiNi_{0.5}Mn_{1.5}O_4$ spinel is their ability to be charged at high current densities and discharged slowly. This is interesting as they approach the requirements of commercial batteries. This property was tested in a spinel prepared in the presence of PEG and calcined at 800°C; cells were charged under two fast regimes (2C and 4C) and further discharged under one slow regime (C/4). Figure 10(a) shows the variation of the capacity as a function of the number of cycles. As can be seen, capacity retention by the cells was quite good (the capacity faded less than 5% after fifty cycles). Moreover, the coulombic efficiency approached 100% upon cycling (see Figure 10(b)). Therefore, the spinel exhibited an excellent electrochemical response under such drastic operating conditions.

3.2.4. *Nanometric $LiNi_{0.5}Mn_{1.5}O_4$ versus $Li_4Ti_5O_{12}$ (hybrid batteries)*

The electrochemical properties of $LiNi_{0.5}Mn_{1.5}O_4$ spinel versus $Li_4Ti_5O_{12}$ were also studied. Figure 11 shows the charge/discharge curves obtained in the 1st, 5th, and 10th cycles for the two types of hybrid batteries examined, with electrodes made from nano (n)- and microparticles (m). All cells were cycled at C/4. The shape of the curves of the cells made from nanometric particles was similar to that observed for the $LiNi_{0.5}Mn_{1.5}O_4$/Li half cell (viz. two pseudoplateaux between 3.0 and 3.3 V associated to the $Ni^{2+} \rightarrow Ni^{4+}$ process, the mechanism of which involves two cubic/cubic two-phase reactions [32]). By contrast, the first charge and discharge curve for the micrometric sample exhibited a third plateau at ca. 2.5 V. This signal is comparable to that for the hybrid cell made from $LiMn_2O_4$ (see Figure 6). For this reason, it

Table 3: Capacity values delivered by the hybrid batteries (mAh/g).

Battery	1st discharge	5th discharge	10th discharge
n-LNMO−n-LTO	110	116	111
m-LNMO−m-LTO	128	120	95

can be assigned to the oxidation of Mn^{3+} to Mn^{4+}. The XRD pattern (not shown here) revealed the presence of NiO related impurities; this means that not all Ni substitutes Mn in the spinel framework, hence the presence of some Mn^{3+} in the spinel framework. The presence of impurities in this spinel is a common finding when the solid is obtained using a conventional ceramic method [33]. The low-voltage plateau disappeared after the second cycle because of the excess of cathode material, and the curve shape was comparable with that for the cells made from nanometric particles except that the two pseudoplateaux were more ill-defined.

The discharge capacities delivered by the cells are shown in Table 3. Except for the capacity value obtained in the first discharge for the cell made from nanometric materials (110 mAh/g which is somewhat lower than that calculated from the spinel stoichiometry) the remaining data exhibited a well-defined trend. Thus, the capacity of the n-LNMO−n-LTO hybrid battery was retained on cycling (at least over the ten cycles measured). This behaviour is similar to that of the n-LMO−n-LTO hybrid battery at the same rate (C/4) (see Table 2). By contrast, the trend exhibited by the capacity of the cell made from micrometric particles is to significantly fade on cycling, consistent with the results for the m-LMO−m-LTO hybrid battery (see Table 2). Again, the performance of the cell made from nanometric particles was better than that of the cell obtained from micrometric particles.

ACKNOWLEDGMENTS

This work was supported by CICYT (MAT2005-03069) and Junta de Andalucía (Group FQM 175).

REFERENCES

[1] A. S. Aricò, P. Bruce, B. Scrosati, J.-M. Tarascon, and W. van Schalkwijk, "Nanostructured materials for advanced energy conversion and storage devices," *Nature Materials*, vol. 4, no. 5, pp. 366–377, 2005.

[2] C. R. Sides, N. Li, C. J. Patrissi, B. Scrosati, and C. R. Martin, "Nanoscale materials for lithium-ion batteries," *MRS Bulletin*, vol. 27, no. 8, pp. 604–607, 2002.

[3] C. R. Sides and C. R. Martin, "Nanostructured electrodes and the low-temperature performance of Li-ion batteries," *Advanced Materials*, vol. 17, no. 1, pp. 125–128, 2005.

[4] C. Jiang, E. Hosono, and H. Zhou, "Nanomaterials for lithium ion batteries," *Nano Today*, vol. 1, no. 4, pp. 28–33, 2006.

[5] L. F. Nazar, G. Goward, F. Leroux, et al., "Nanostructured materials for energy storage," *International Journal of Inorganic Materials*, vol. 3, no. 3, pp. 191–200, 2001.

[6] A. Singhal, G. Skandan, G. Amatucci, et al., "Nanostructured electrodes for next generation rechargeable electrochemical devices," *Journal of Power Sources*, vol. 129, no. 1, pp. 38–44, 2004.

[7] F. F. C. Bazito and R. M. Torresi, "Cathodes for lithium ion batteries: the benefits of using nanostructured materials," *Journal of the Brazilian Chemical Society*, vol. 17, no. 4, pp. 627–642, 2006.

[8] J. C. Arrebola, A. Caballero, L. Hernán, J. Morales, E. Rodríguez-Castellón, and J. R. Ramos Barrado, "Effects of coating with gold on the performance of nanosized $LiNi_{0.5}Mn_{1.5}O_4$ for lithium batteries," *Journal of the Electrochemical Society*, vol. 154, no. 3, pp. A178–A184, 2007.

[9] M. S. Whittingham, "Lithium batteries and cathode materials," *Chemical Reviews*, vol. 104, no. 10, pp. 4271–4301, 2004.

[10] M. M. Thackeray, "Manganese oxides for lithium batteries," *Progress in Solid State Chemistry*, vol. 25, no. 1-2, pp. 1–71, 1997.

[11] L. Hernán, J. Morales, L. Sánchez, J. Santos, and E. Rodríguez-Castellón, "Sol-gel derived Li-V-Mn-O spinels as cathodes for rechargeable lithium batteries," *Solid State Ionics*, vol. 133, no. 3-4, pp. 179–188, 2000.

[12] C. Sigala, D. Guyomard, A. Verbaere, Y. Piffard, and M. Tournoux, "Positive electrode materials with high operating voltage for lithium batteries: $LiCr_yMn_{2-y}O_4 (0 \leq y \leq 1)$," *Solid State Ionics*, vol. 81, no. 3-4, pp. 167–170, 1995.

[13] H. Kawai, M. Nagata, M. Tabuchi, H. Tukamoto, and A. R. West, "Novel 5 V spinel cathode $Li_2FeMn_3O_8$ for lithium ion batteries," *Chemistry of Materials*, vol. 10, no. 11, pp. 3266–3268, 1998.

[14] H. Kawai, M. Nagata, H. Tukamoto, and A. R. West, "A new lithium cathode $LiCoMnO_4$: toward practical 5 V lithium batteries," *Electrochemical and Solid-State Letters*, vol. 1, no. 5, pp. 212–214, 1998.

[15] Y. Ein-Eli, W. F. Howard Jr., S. H. Lu, et al., "$LiMn_{2-x}Cu_xO_4$ spinels ($0.1 \leq x \leq 0.5$): a new class of 5 V cathode materials for Li batteries. I. Electrochemical, structural, and spectroscopic studies," *Journal of the Electrochemical Society*, vol. 145, no. 4, pp. 1238–1244, 1998.

[16] Q. Zhong, A. Bonakdarpour, M. Zhang, Y. Gao, and J. R. Dahn, "Synthesis and electrochemistry of $LiNi_xMn_{2-x}O_4$," *Journal of the Electrochemical Society*, vol. 144, no. 1, pp. 205–213, 1997.

[17] M. G. Lazarraga, L. Pascual, H. Gadjov, et al., "Nanosize $LiNi_yMn_{2-y}O_4$ ($0 < y \leq 0.5$) spinels synthesized by a sucrose-aided combustion method. Characterization and electrochemical performance," *Journal of Materials Chemistry*, vol. 14, no. 10, pp. 1640–1647, 2004.

[18] X. R. Ye, D. Z. Jia, J. Q. Yu, X. Q. Xin, and Z. Xue, "One-step solid-state reactions at ambient temperatures—a novel approach to nanocrystals synthesis," *Advanced Materials*, vol. 11, no. 11, pp. 941–942, 1999.

[19] J. C. Arrebola, A. Caballero, M. Cruz, L. Hernán, J. Morales, and E. Rodríguez-Castellón, "Crystallinity control of a nanostructured $LiNi_{0.5}Mn_{1.5}O_4$ spinel via polymer-assisted synthesis: a method for improving its rate capability and performance in 5 V lithium batteries," *Advanced Functional Materials*, vol. 16, no. 14, pp. 1904–1912, 2006.

[20] A. Odani, A. Nimberger, B. Markovsky, et al., "Development and testing of nanomaterials for rechargeable lithium batteries," *Journal of Power Sources*, vol. 119–121, pp. 517–521, 2003.

[21] A. Caballero, M. Cruz, L. Hernán, M. Melero, J. Morales, and E. Rodríguez-Castellón, "Nanocrystalline materials obtained by using a simple, rapid method for rechargeable lithium batteries," *Journal of Power Sources*, vol. 150, pp. 192–201, 2005.

[22] G. Armstrong, A. R. Armstrong, P. Bruce, P. Reale, and B. Scrosati, "TiO_2(B) nanowires as an improved anode

material for lithium-ion batteries containing $LiFePO_4$ or $LiNi_{0.5}Mn_{1.5}O_4$ cathodes and a polymer electrolyte," *Advanced Materials*, vol. 18, no. 19, pp. 2597–2600, 2006.

[23] H. P. Klug and L. E. Alexander, *X-Ray Diffraction Procedures for Pollycrystalline and Amorphous Materials*, John Willey & Sons, New York, NY, USA, 1974.

[24] W. A. Rachinger, "A correction for the $\alpha_1\alpha_2$ doublet in the measurement of widths of x-ray diffraction lines," *Journal of Scientific Instruments*, vol. 25, no. 7, pp. 254–255, 1948.

[25] M. Winter, J. O. Besenhard, M. E. Spahr, and P. Novák, "Insertion electrode materials for rechargeable lithium batteries," *Advanced Materials*, vol. 10, no. 10, pp. 725–763, 1998.

[26] L. Kavan and M. Grätzel, "Facile synthesis of nanocrystalline $Li_4Ti_5O_{12}$ (spinel) exhibiting fast Li insertion," *Electrochemical and Solid-State Letters*, vol. 5, no. 2, pp. A39–A42, 2002.

[27] J. C. Arrebola, A. Caballero, and L. Hernán, "High performance hybrid lithium-ion batteries based on combinations of nanometric materials," *Nanotechnology*, vol. 18, no. 29, Article ID 295705, 5 pages, 2007.

[28] A. Ott, P. Endres, V. Klein, et al., "Electrochemical performance and chemical properties of oxidic cathode materials for 4 V rechargeable Li-ion batteries," *Journal of Power Sources*, vol. 72, no. 1, pp. 1–8, 1998.

[29] Y. Terada, K. Yasaka, F. Nishikawa, T. Konishi, M. Yoshio, and I. Nakai, "*In situ* XAFS analysis of $Li(Mn, M)_2O_4$ (M = Cr, Co, Ni) 5 V cathode materials for lithium-ion secondary batteries," *Journal of Solid State Chemistry*, vol. 156, no. 2, pp. 286–291, 2001.

[30] J. C. Arrebola, A. Caballero, L. Hernán, and J. Morales, "Expanding the rate capabilities of the $LiNi_{0.5}Mn_{1.5}O_4$ spinel by exploiting the synergistic effect between nano and microparticles," *Electrochemical and Solid-State Letters*, vol. 8, no. 12, pp. A641–A645, 2005.

[31] Z. Zhang, A. J. Rondinone, J. X. Ma, J. Shen, and S. Dai, "Morphologically templated growth of aligned spinel $CoFe_2O_4$ nanorods," *Advanced Materials*, vol. 17, no. 11, pp. 1415–1419, 2005.

[32] K. Ariyoshi, Y. Iwakoshi, N. Nakayama, and T. Ohzuku, "Topotactic two-phase reactions of $Li[Ni_{1/2}Mn_{3/2}]O_4(P4_332)$ in nonaqueous lithium cells," *Journal of the Electrochemical Society*, vol. 151, no. 2, pp. A296–A303, 2004.

[33] Y. Ein-Eli, J. T. Vaughey, M. M. Thackeray, S. Mukerjee, X. Q. Yang, and J. McBreen, "$LiNi_xCu_{0.5-x}Mn_{1.5}O_4$ spinel electrodes, superior high-potential cathode materials for Li batteries. I. Electrochemical and structural studies," *Journal of the Electrochemical Society*, vol. 146, no. 3, pp. 908–913, 1999.